CME SAM

Lung CT

AJR FOCUS ON:

Lung CT: Part 1, Mimickers of Lung Cancer—Spectrum of CT Findings With Pathologic Correlation

Kiyomi Furuya[1]
Kotaro Yasumori[1]
Sadanori Takeo[2]
Ikuo Sakino[3]
Noriko Uesugi[4]
Seiya Momosaki[5]
Toru Muranaka[1]

OBJECTIVE. The purpose of this article is to describe CT findings of miscellaneous pulmonary conditions that mimic lung cancers, especially primary cancers, to improve diagnosis of pulmonary lesions. Brief descriptions of patient clinical information and pathologic findings will be included and correlated with imaging findings in actual cases.

CONCLUSION. A wide variety of pulmonary conditions present imaging features that mimic those of primary lung cancers and are difficult to differentiate from cancer. Awareness of these conditions with an understanding of their pathologic background and careful attention to the clinical information will help achieve correct diagnoses.

Keywords: ground-glass opacity, high-resolution CT, inflammatory nodule, lung cancer, nonneoplastic pulmonary disease

DOI:10.2214/AJR.10.7262

Received June 1, 2010; accepted after revision February 3, 2012.

[1]Department of Radiology and Clinical Research Institute, National Hospital Organization Kyushu Medical Center, 1-8-1 Gigyohama Chuouku, Fukuoka 810-8563, Japan. Address correspondence to K. Furuya (kymfuruya@me.com).

[2]Division of General Thoracic Surgery, Respiratory Clinical and Research Center, National Hospital Organization Kyushu Medical Center, Fukuoka, Japan.

[3]Department of Radiology, Saiseikai Yahata General Hospital, Fukuoka, Japan.

[4]Department of Molecular Pathology, Graduate School of Comprehensive Human Science, University of Tsukuba, Ibaraki, Japan.

[5]Department of Pathology, National Hospital Organization Kyushu Medical Center, Fukuoka, Japan.

CME/SAM
This article is available for CME/SAM credit.

WEB
This is a Web exclusive article.

AJR 2012; 199:W454–W463

0361–803X/12/1994–W454

Great improvement in CT, especially in high-resolution CT (HRCT) and MDCT with isotropic volumetric CT examination, has made it possible to show precisely the morphologic characteristics of a disease and, thus, make correct imaging diagnoses of lung cancer possible in many cases [1–3]. However, miscellaneous conditions produce CT findings that mimic those of primary cancers, and differentiating their imaging findings from cancers still remains difficult, even with the current CT techniques [4]. In this article, we will discuss these pulmonary conditions that mimic primary lung cancers. The clinical conditions and their pathologic correlations of actual cases will also be described.

Pulmonary conditions can be grossly classified into three categories: ground-glass opacification (GGO; both pure and mixed), solid nodules and masses, and consolidation on HRCT. We will focus on GGO and solid nodules and masses in this article because clinical difficulties in the differentiation of the benignity or malignancy of a pulmonary lesion occur much more frequently in these two types than with consolidative diseases.

Ground-Glass Opacification

GGO is defined as a hazy opacity that preserves underlying bronchial and vascular margins on HRCT [5, 6]. Nonneoplastic GGO is caused by partial airspace filling, interstitial thickening with inflammation, edema, fibrosis, partial collapse of alveoli, or focal hemorrhage [7, 8]. Neoplastic GGO results mainly from alveolar wall covering tumor growth or hemorrhagic tumor [8, 9]. GGO can be classified into pure GGO and halo or mixed GGO types according to the presence or absence of solid components. The halo sign represents the ground-glass opacity surrounding the circumference of a nodule or mass [5, 6]. A mixed GGO is a nodule that has both GGO and solid components.

Pure GGO

Adenocarcinoma in situ (nonmucinous type) shows pure GGO on HRCT (Fig. 1). Differential diagnosis of it includes atypical adenomatous hyperplasia, focal fibrosis, pulmonary hemorrhage, and acute inflammation [8, 10–12].

Atypical adenomatous hyperplasia—Atypical adenomatous hyperplasia (AAH) is a peripheral focal lesion produced by proliferation of atypical cuboidal or columnar epithelial cells along the alveoli and respiratory bronchioles [13, 14]. AAH is a putative precursor of adenocarcinoma, including adenocarcinoma in situ [14]. It presents as a round or oval pure GGO nodule without pleural indentation or vascular convergence. AAH is usually smaller than 5 mm in diameter, though it may be as large as 10–17 mm, and is indistinguishable from nonmucinous adenocarcinoma in situ that manifests as pure GGO on HRCT [10–12, 15] (Fig. 2).

Focal fibrosis—Focal fibrosis is a benign nonneoplastic disease often manifesting as a GGO that sometimes retains the same configuration

over a long period and often produces the same imaging findings as neoplastic GGO [8, 10, 12, 16]. It presents as GGO with a round, polygonal, spiculated, or ill-defined margin on HRCT [17]. Pathologically, it appears as a focal interstitial septal thickening with fibroblast proliferation and preservation of alveolar airspaces and macrophage-filled alveoli [12, 17] (Fig. 3).

Halo or Mixed GGO

In nonneoplastic lesions, these patterns are mainly seen in cases with hemorrhagic nodules, such as invasive aspergillosis and Wegener granulomatosis [9] (Fig. 4). The lesions are difficult to distinguish from a minimally invasive adenocarcinoma, with a halo sign or mixed GGO on HRCT resulting from predominant lepidic tumor growth (Fig. 5). Careful attention to the patient's clinical information will help in making the correct diagnosis.

Solid Nodules and Masses

The main pulmonary conditions that manifest as solid nodules and masses mimicking lung cancer are neoplastic (e.g., hamartoma, pneumocytoma [sclerosing hemangioma], inflammatory myofibroblastic tumor, and lymphoma) and nonneoplastic (e.g., intrapulmonary lymph node, tumorlet, tuberculoma, histoplasmoma, rounded atelectasis, amyloidosis, focal organizing pneumonia, and lung abscess).

Hamartoma

Hamartoma is a benign neoplasm composed of mesenchymal tissues such as cartilage, fat, connective tissue, smooth muscle, and calcification. Pathologically, it sometimes shows slitlike clefts lined by entrapped ciliated epithelium. Hamartoma accounts for 6–8% of solitary lung tumors and 77% of all benign tumors [18, 19]. Typical CT findings consist of a well-defined, smooth, round, or lobulated nodule or mass [20]. Fat is recognized on the CT image in about 60% of cases, and popcornlike calcification or central calcification in about 25% [20]. A hamartoma with little fat and no calcification is difficult to distinguish on CT from primary lung cancer with a round or lobulated margin (Fig. 6).

Pneumocytoma (Sclerosing Hemangioma)

Pneumocytoma is a rare benign tumor predominantly found in middle-aged women. The female-to-male ratio is approximately 4–5:1 [21]. Histologically, the essence is proliferation of type 2 pneumocytes, and a pneumocytoma consists of four major histologic components: solid, papillary, sclerotic, and hemangiomatous [13]. Though low-attenuation areas, calcification, and, rarely, air-meniscus sign are sometimes present on CT, most cases usually show a smoothly marginated, homogeneously well-enhanced, round, or oval nodule or mass, and differentiation from solid lung cancer with round or oval margins is difficult on CT [22, 23] (Fig. 7). Histologic confusion with adenocarcinoma with lepidic tumor growth also occurs occasionally, with specimens obtained from not only transbronchial lung biopsy but also frozen sections, especially when the specimen contains only papillary components [24].

Inflammatory Myofibroblastic Tumor

Because of its variable cellular components, inflammatory myofibroblastic tumor (IMT) has been described by various terms, including inflammatory pseudotumor, fibrous histiocytoma, xanthogranuloma, and plasma cell granuloma [13]. It is an uncommon lesion composed of spindle myofibroblasts on a variable background of collagen and inflammatory cells [13]. The spindle cell components express vimentin and α-smooth muscle actin on immunostaining. Although it has a wide spectrum of benign reactive-to-malignant characteristics and the true nature of these lesions has not been fully elucidated, the expression of anaplastic lymphoma kinase 1 in about 56% of cases suggests that they may be neoplastic [25, 26].

IMT is most frequently found in the lung [13]. Endobronchial or endotracheal lesions occur occasionally, and it can occur in all other organs. Though it occurs at all ages, it frequently is found in children and adults younger than 40 years [13]. Most patients are asymptomatic, but sometimes patients present with cough, hemosputum, and sometimes a history of previous infection. Most cases of IMT are diagnosed and cured by surgical resection. The prognosis is excellent. Overall survival at 5 years is 91%, although relapse has been reported in patients who underwent incomplete resection [27]. The tumor usually manifests as a well-defined lobulated or round solitary peripheral pulmonary nodule or mass on CT [28]. It occasionally shows consolidation or a nodule with an ill-defined margin or spiculations mimicking lung cancer [28]. The internal structure is homogeneous or heterogeneous with hemorrhage, necrosis, and calcification, and shows varying degrees of contrast enhancement [29]. The varied CT manifestations make it difficult to make a correct imaging diagnosis (Fig. 8).

Intrapulmonary Lymph Node

Intrapulmonary lymph nodes are commonly found in the pulmonary hilum, but they can also occur within the lung parenchyma, most commonly in the subpleural zone of the lower lobes [30, 31]. They are often found in smokers.

As CT has improved and more CT examinations have been performed, incidental intrapulmonary lymph nodes have been found more often. They are usually a single nodule smaller than 10 mm in diameter, with 10% of cases having two or more lesions [30]. Pathologically, they are normal lymph nodes with a capsule and lymphoid follicles [30, 32]. Though they commonly present as well-defined oval nodules (Fig. 9), sometimes they show spiculations, pleural indentation, fuzzy margin, and vascular involvement, mimicking primary lung cancer [32]. Though they usually remain the same size for many years, a few cases grow rapidly and are difficult to differentiate from cancer [33].

Pulmonary Tumorlets

Pulmonary tumorlets refer to a minute nodular proliferation of airway neuroendocrine cells (Kulchitsky cells) that extends beyond the epithelium into the adjacent wall or lung parenchyma [13, 34]. Histologically, a tumorlet consists of nests of oval to spindle-shaped cells. Neuroendocrine granules are seen on electron microscopy, and polypeptides similar to those in carcinoid are present in the tumorlet. It has a benign nonneoplastic nature. It is often associated with damaged and ectatic small airways or carcinoid tumor itself and ranges in size from microscopic to 5–8 mm in diameter. A nodule bigger than this size should be considered a carcinoid. Because of their minute size, they are not usually apparent on CT but are found incidentally at histopathologic examination, frequently as multiple tiny lesions. If visualized on HRCT, they show well-defined tiny nodules and are difficult to differentiate from cancer, especially from metastatic cancer in the case of multiple lesions [35] (Fig. 10).

Tuberculoma and Histoplasmoma

Pulmonary tuberculosis may present as an asymptomatic solitary pulmonary nodule called a tuberculoma, and histoplasmosis may present as a histoplasmoma in immunocompetent patients [36]. They sometimes mimic lung cancer.

A tuberculoma is a well-defined round or oval focus of parenchymal tuberculosis [36]. Sometimes calcification and cavitation in the

nodule or satellite nodules can be seen and help in the imaging diagnosis [36, 37]. Pathologically, the central region of the tuberculoma consists of caseous necrosis and a marginal zone of epithelioid granuloma, inflammatory cells, and collagen. Tuberculomas show a variable contrast-enhancement pattern, depending on the inflammatory process on contrast-enhanced CT, though most of them show a central low-attenuation area surrounded by ring enhancement, reflecting central necrosis and granulomatous inflammatory tissue in the outer zone [38, 39]. This CT enhancement pattern is also found in lung cancer with necrosis. Tuberculomas most commonly appear as smoothly marginated round nodules on CT [36, 37]. However, tuberculomas sometimes have spiculated margins, especially when the background parenchyma is emphysematous or fibrotic, making them difficult to distinguish from cancer with fine spiculations [4, 36] (Fig. 11).

Histoplasmoma is a chronic form of pulmonary histoplasmosis caused by the fungus *Histoplasma capsulatum* that may or may not be associated with a history of symptomatic disease [36]. It usually is seen as a sharply defined nodule. It may have a central zone of calcification, may be diffusely calcified, or may be accompanied by small satellite nodules that resemble a tuberculoma [36, 40]. The presence of central or diffuse calcification in a nodule 3 cm or smaller in diameter is virtually diagnostic of a granuloma [36]. In an area where histoplasmosis is endemic, *H. capsulatum* is the most likely cause; however, in the absence of calcification, the differential diagnosis must include all other causes of solitary or multiple nodules, including primary lung cancer [36, 40, 41]. Occasionally, a histoplasmoma shows shaggy or irregular edge mimicking lung cancer [40].

Rounded Atelectasis

Rounded atelectasis is a focal pleural-based lesion that is the result of pleural and subpleural scarring and atelectasis of the adjacent lung tissue [42]. It occurs most often in the dorsal subpleural regions of the lower lobe in patients with a history of asbestos exposure and in patients with tuberculosis [42]. Pathologic examinations show pleural fibrosis overlying the abnormal parenchyma, as well as invaginations of fibrotic pleura into the collapsed parenchyma. Characteristic CT findings consist of a round mass at the lung base adjacent to the pleural thickening and a comet-tail sign—that is, vessels and bronchi converge on and swirl around the mass. It may appear as an air bronchogram [43]. It sometimes shows a mass with a wedge-shaped or irregular margin on CT that is confused with a malignant tumor (Fig. 12). Correct diagnosis is very important, especially in patients exposed to asbestos owing to the increased incidence of malignant mesothelioma and lung cancer. Good homogeneous enhancement on contrast-enhanced CT is a clue for differentiating it from malignancy [44]. Fluorine-18-FDG PET can also help in correct diagnosis because the atelectasis found is most commonly metabolically inactive [45].

Pulmonary Amyloidosis

Amyloidosis is the accumulation of various abnormal insoluble fibrillar proteins (amyloid) in the extracellular space. The most frequent amyloid found in the lung is amyloid light chain [46]. Amyloidosis can affect the lung as either a primary or secondary type, and as a systemic type or as a disease limited to the lung. Amyloidosis that manifests primarily in the lower respiratory tract can be divided into three types: tracheobronchial, nodular parenchymal, and diffuse parenchymal (also termed alveolar septal) amyloidosis. Nodular parenchymal amyloidosis presents as a single or multiple peripheral pulmonary nodules in a wide variety of sizes with a round, lobulated, serrated, or spiculated margin [47]. Cavitation is seen in up to 20% of cases and calcification is seen in 20–50% on CT scans [47]. It may grow very slowly over years. Poor enhancement on contrast-enhanced CT is reported in cases of pulmonary amyloidosis [48]. Usually, patients with nodular amyloidosis are asymptomatic. Differentiation from lung cancer on CT is difficult, especially in cases with an uncalcified solitary nodule with an irregular margin [47, 48] (Fig. 13). Low signal intensity on T2-weighted MRI resulting from a short T2 relaxation time due to amyloid protein may help in the diagnosis [48].

Lung Abscess

Lung abscess is often associated with bacterial pneumonia or is preceded by aspiration. The organisms are often anaerobic bacteria, including *Klebsiella pneumonia*, *Pseudomonas aeruginosa*, *Staphylococcus aureus*, and *Nocardia* and *Actinomyces* species [49]. Aspiration occurs especially in patients with alcoholism, mental retardation, poor dental hygiene, and immune suppression [36, 49]. Imaging findings comprise single or multiple lung masses or nodules, often with cavities, which are sometimes subsolid in the chronic phase [36, 49]. They may be isolated or occur within areas of consolidation [36, 40]. In most cases, the walls of the cavities are smooth and less than 15 mm thick [36, 50]. An irregular and thick wall (> 15 mm) is occasionally seen and, in such cases, it resembles cavitated lung cancer [50]. Lung abscess may also manifest as a nonspecific consolidation or nodular opacity, and differentiation from cancer is challenging in the latter case [4] (Fig. 14).

Focal Organizing Pneumonia

Focal organizing pneumonia is referred to as unresolving pneumonia or pneumonia with a delayed resolution, but there is no clear clinical definition [51]. It consists histologically of polypoid granulation tissue in the alveolar spaces and peripheral bronchial lumen associated with chronic inflammatory infiltrate [51].

It shows a wide variety of CT findings. Usually, it shows consolidation. On the other hand, focal organizing pneumonia may present as a nodule with an oval or spindle-shaped margin and satellite lesions. Sometimes the CT images of focal organizing pneumonia show a nodule with a spiculated margin, air bronchogram, bubblelike lucency, halo sign, mixed GGO, and pleural indentation resembling primary lung cancer [52, 53]. Differentiation from lung cancer is difficult, and many patients undergo surgery in such cases [52, 53]. Not only in focal organizing pneumonia but also in other inflammatory nodules as well, the margins are sometimes concave with a few rough spiculations [4]. One report postulated that retraction of the affected lobule, in contrast to intact adjacent lobules, causes a concave margin in the healing process of the inflammation [54]. It sometimes mimics primary lung cancer with spiculated margin [4]. The differentiation between such inflammatory nodules and lung cancer is difficult [4, 52, 53] (Fig. 15).

Lymphoma

Primary lymphoma of the lung is rare. Most are marginal zone B cell lymphomas arising from mucosal-associated lymphoid tissue lymphoma, which is categorized as a low-grade malignancy [13]. Formerly referred to as "pseudolymphoma," this category is now considered to consist of mucosal-associated lymphoid tissue lymphoma, nodular lymphoid hyperplasia, and other low-grade lymphoproliferative disorders [13, 55, 56].

Secondary pulmonary lymphoma occurs more frequently than primary lymphoma. A

wide variety of CT findings are found in primary and secondary lymphoma: single or multiple pulmonary nodules and masses, consolidation, GGO, air bronchogram, cavities, and peribronchovascular thickening [55, 56]. Sometimes lymphoma manifests as a nodule or mass resembling a primary or metastatic lung cancer in the CT images [55–57] (Fig. 16).

Conclusion

A wide variety of pulmonary conditions produce radiologic findings that mimic lung cancers. Understanding these conditions and their pathologic backgrounds combined with careful attention to the clinical information will help in making correct diagnoses.

References

1. Murata K, Khan A, Herman PG. Pulmonary parenchymal disease: evaluation with high-resolution CT. *Radiology* 1989; 170:629–635
2. Zwirewich CV, Vedal S, Miller RR, Müller NL. Solitary pulmonary nodule: high-resolution CT and radiologic-pathologic correlation. *Radiology* 1991; 179:469–476
3. Beigelman-Aubry C, Hill C, Guibal A, Savatovsky J, Grenier PA. Multi-detector row CT and postprocessing techniques in the assessment of diffuse lung disease. *RadioGraphics* 2005; 25:1639–1652
4. Furuya K, Murayama S, Soeda H, et al. New classification of small pulmonary nodules by margin characteristics on high-resolution CT. *Acta Radiol* 1999; 40:496–504
5. Austin JH, Müller NL, Friedman PJ, et al. Glossary of terms for CT of the lungs: recommendations of the Nomenclature Committee of the Fleischner Society. *Radiology* 1996; 200:327–331
6. Hansell DM, Bankier AA, MacMahon H, McLoud TC, Müller NL, Remy J. Fleischner Society: glossary of terms for thoracic imaging. *Radiology* 2008; 246:697–722
7. Remy-Jardin M, Remy J, Giraud F, Wattinne L, Gosselin B. Computed tomography assessment of ground-glass opacity: semiology and significance. *J Thorac Imaging* 1993; 8:249–264
8. Park CM, Goo JM, Lee HJ, Lee CH, Chun EJ, Im JG. Nodular ground-glass opacity at thin-section CT: histologic correlation and evaluation of change at follow-up. *RadioGraphics* 2007; 27:391–408
9. Primack SL, Hartman TE, Lee KS, Müller NL. Pulmonary nodules and the CT halo sign. *Radiology* 1994; 190:513–515
10. Kim HY, Shim YM, Lee KS, Han J, Yi CA, Kim YK. Persistent pulmonary nodular ground-glass opacity at thin-section CT: histopathologic comparisons. *Radiology* 2007; 245:267–275
11. Nakata M, Saeki H, Takata I, et al. Focal ground-glass opacity detected by low-dose helical CT. *Chest* 2002; 121:1464–1467
12. Nakajima R, Yokose T, Kakinuma R, Nagai K, Nishiwaki Y, Ochiai A. Localized pure ground-glass opacity on high-resolution CT: histologic characteristics. *J Comput Assist Tomogr* 2002; 26:323–329
13. Travis W, Brambilla E, Müller-Hermelink HK, Harris CC. Tumors of the lung. In: Travis W, Brambilla E, Müller-Hermelink HK, Harris CC, eds. *Pathology and genetics of tumours of the lung, pleura, thymus and heart*. Lyon, France: IARC Press, 2004:9–124
14. Shimamoto Y, Kodama T, Kameya T. Morphogenesis of peripheral type adenocarcinoma of the lung. In: Shimamoto Y, Melamed MR, Nettesheim P, eds. *Morphogenesis of lung cancer.* Boca Raton: CRC Press, 1982:65–90
15. Kawakami S, Sone S, Takashima S, et al. Atypical adenomatous hyperplasia of the lung: correlation between high-resolution CT findings and histopathologic features. *Eur Radiol* 2001; 11:811–814
16. Takashima S, Sone S, Li F, et al. Small solitary pulmonary nodules (< or =1 cm) detected at population-based CT screening for lung cancer: reliable high-resolution CT features of benign lesions. *AJR* 2003; 180:955–964
17. Park CM, Goo JM, Lee HJ, et al. Focal interstitial fibrosis manifesting as nodular ground-glass opacity: thin-section CT findings. *Eur Radiol* 2007; 17:2325–2331
18. Bateson EM. An analysis of 155 solitary lung lesions illustrating the differential diagnosis of mixed tumours of the lung. *Clin Radiol* 1965; 16:51–65
19. Hansen CP, Holtveg H, Francis D, Rasch L, Bertelsen S. Pulmonary hamartoma. *J Thorac Cardiovasc Surg* 1992; 104:674–678
20. Siegelman SS, Khouri NF, Scott WWJ, et al. Pulmonary hamartoma: CT findings. *Radiology* 1986; 160:313–317
21. Sugio K, Yokoyama H, Kaneko S, Ishida T, Sugimachi K. Sclerosing hemangioma of the lung: radiographic and pathological study. *Ann Thorac Surg* 1992; 53:295–300
22. Im JG, Kim WH, Han MC, et al. Sclerosing hemangiomas of the lung and interlobar fissures: CT findings. *J Comput Assist Tomogr* 1994; 18:34–38
23. Wang QB, Chen YQ, Shen JJ, et al. Sixteen cases of pulmonary sclerosing haemangioma: CT findings are not definitive for preoperative diagnosis. *Clin Radiol* 2011; 66:708–714
24. Mikuz G, Szinicz G, Fischer H. Sclerosing angioma of the lung: case report and electron microscope investigation. *Virchows Arch A Pathol Anat Histol* 1979; 385:93–101
25. Coffin CM, Patel A, Perkins S, Elenitoba-Johnson KS, Perlman E, Griffin CA. ALK1 and p80 expression and chromosomal rearrangements involving 2p23 in inflammatory myofibroblastic tumor. *Mod Pathol* 2001; 14:569–576
26. Coffin CM, Hornick JL, Fletcher CD. Inflammatory myofibroblastic tumor: comparison of clinicopathologic, histologic, and immunohistochemical features including ALK expression in atypical and aggressive cases. *Am J Surg Pathol* 2007; 31:509–520
27. Cerfolio RJ, Allen MS, Nascimento AG, et al. Inflammatory pseudotumors of the lung. *Ann Thorac Surg* 1999; 67:933–936
28. Agrons GA, Rosado-de-Christenson ML, Kirejczyk WM, Conran RM, Stocker JT. Pulmonary inflammatory pseudotumor: radiologic features. *Radiology* 1998; 206:511–518
29. Kim TS, Han J, Kim GY, Lee KS, Kim H, Kim J. Pulmonary inflammatory pseudotumor (inflammatory myofibroblastic tumor): CT features with pathologic correlation. *J Comput Assist Tomogr* 2005; 29:633–639
30. Bankoff MS, McEniff NJ, Bhadelia RA, Garcia-Moliner M, Daly BD. Prevalence of pathologically proven intrapulmonary lymph nodes and their appearance on CT. *AJR* 1996; 167:629–630
31. Oshiro Y, Kusumoto M, Moriyama N, et al. Intrapulmonary lymph nodes: thin-section CT features of 19 nodules. *J Comput Assist Tomogr* 2002; 26:553–557
32. Tsunezuka Y, Sato H, Hiranuma C, et al. Intrapulmonary lymph nodes detected by exploratory video-assisted thoracoscopic surgery: appearance of helical computed tomography. *Ann Thorac Cardiovasc Surg* 2000; 6:369–372
33. Nagahiro I, Andou A, Aoe M, Date H, Shimizu N. Intrapulmonary lymph nodes enlarged after lobectomy for lung cancer. *Ann Thorac Surg* 2001; 72:2115–2117
34. Fraser RS, Müller NL, Colman N, Pare PD. Pulmonary neoplasms. In: Fraser RS, Müller NL, Colman N, Pare PD, eds. *Fraser and Pare's diagnosis of diseases of the chest*, 4th ed. Philadelphia, PA: Saunders, 1999:1067–1417
35. Ginsberg MS, Akin O, Berger DM, Zakowski MF, Panicek DM. Pulmonary tumorlets: CT findings. *AJR* 2004; 183:293–296
36. Fraser RS, Müller NL, Colman N, Pare PD. Pulmonary infection. In: Fraser RS, Müller NL, Colman N, Pare PD, eds. *Fraser and Pare's diagnosis of diseases of the chest*, 4th ed. Philadelphia, PA: Saunders, 1999:695–1066
37. Lee KS, Im JG. CT in adults with tuberculosis of the chest: characteristic findings and role in management. *AJR* 1995; 164:1361–1367
38. Murayama S, Murakami J, Hashimoto S, Torii Y, Masuda K. Noncalcified pulmonary tuberculomas: CT enhancement patterns with histological correlation. *J Thorac Imaging* 1995; 10:91–95
39. Tateishi U, Kusumoto M, Akiyama Y, Kishi F, Nishimura M, Moriyama N. Role of contrast-enhanced dynamic CT in the diagnosis of active tuberculoma. *Chest* 2002; 122:1280–1284

40. Hansell DM, Lynch DA, McAdams HP, Bankier AA. Infections of the lungs and pleura. In: Hansell DM, Lynch DA, McAdams HP, Bankier AA, eds. *Imaging of diseases of the chest*, 5th ed. St. Louis, MO: Mosby, 2010:205–294
41. Rolston KV, Rodriguez S, Dholakia N, Whimbey E, Raad I. Pulmonary infections mimicking cancer: a retrospective, three-year review. *Support Care Cancer* 1997; 5:90–93
42. Hillerdal G. Rounded atelectasis: clinical experience with 74 patients. *Chest* 1989; 95:836–841
43. Schneider HJ, Felson B, Gonzalez LL. Rounded atelectasis. *AJR* 1980; 134:225–232
44. Hakomäki J, Keski-Nisula L, Paakkala T. Contrast enhancement of round atelectases. *Acta Radiol* 2002; 43:376–379
45. McAdams HP, Erasums JJ, Patz EF, Goodman PC, Coleman RE. Evaluation of patients with round atelectasis using 2-[^{18}F]-fluoro-2-deoxy-D-glucose PET. *J Comput Assist Tomogr* 1998; 22:601–604
46. Chen KT. Amyloidosis presenting in the respiratory tract. *Pathol Annu* 1989; 24:253–273
47. Pickford HA, Swensen SJ, Utz JP. Thoracic cross-sectional imaging of amyloidosis. *AJR* 1997; 168:351–355
48. Matsumoto K, Ueno M, Matsuo Y, Kudo S, Horita K, Sakao Y. Primary solitary amyloidoma of the lung: findings on CT and MRI. *Eur Radiol* 1997; 7:586–588
49. Dail DH. Bronchial and transbronchial diseases. In: Dail DH, Hammar SP, eds. *Pulmonary pathology*, 2nd ed. New York, NY: Springer-Verlag, 1994:79–119
50. Groskin SA, Panicek DM, Ewing DK, et al. Bacterial lung abscess: a review of the radiographic and clinical features of 50 cases. *J Thorac Imaging* 1991; 6:62–67
51. Cordier JF. Organising pneumonia. *Thorax* 2000; 55:318–328
52. Yang PS, Lee KS, Han J, Kim EA, Kim TS, Choo IW. Focal organizing pneumonia: CT and pathologic findings. *J Korean Med Sci* 2001; 16:573–578
53. Kohno N, Ikezoe J, Johkoh T, et al. Focal organizing pneumonia: CT appearance. *Radiology* 1993; 189:119–123
54. Oshita F, Eguchi K, Miya T, et al. Thin-slice CT analysis of localized inflammatory pulmonary lesions: pathologic-CT correlation. *Nippon Igaku Hoshasen Gakkai Zasshi* 1989; 49:1525–1533
55. Wislez M, Cadranel J, Antoine M, et al. Lymphoma of pulmonary mucosa-associated lymphoid tissue: CT scan findings and pathological correlations. *Eur Respir J* 1999; 14:423–429
56. King LJ, Padley SP, Wotherspoon AC, Nicholson AG. Pulmonary MALT lymphoma: imaging findings in 24 cases. *Eur Radiol* 2000; 10:1932–1938
57. Rush WL, Andriko JA, Taubenberger JK, et al. Primary anaplastic large cell lymphoma of the lung: a clinicopathologic study of five patients. *Mod Pathol* 2000; 13:1285–1292

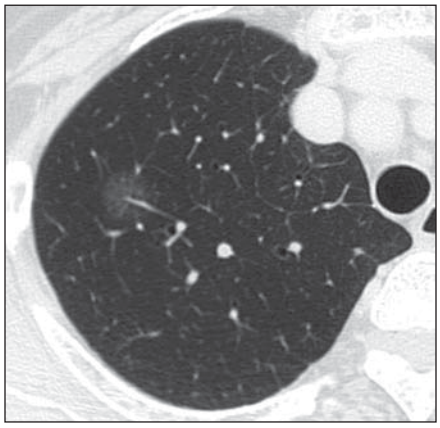

A

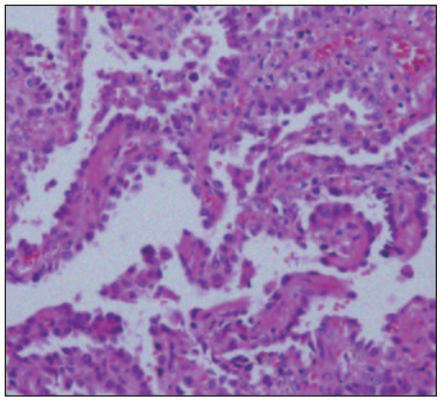

B

Fig. 1—78-year-old woman with adenocarcinoma in situ.
A, Pure ground-glass opacification (diameter, 15 mm) preserving involved pulmonary vessel in right upper lobe is shown on high-resolution CT image.
B, Histologically, tumor cells extend alveolar wall without destruction of underlying lung structures.

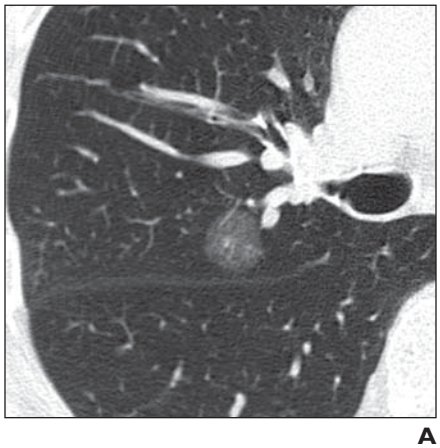

A

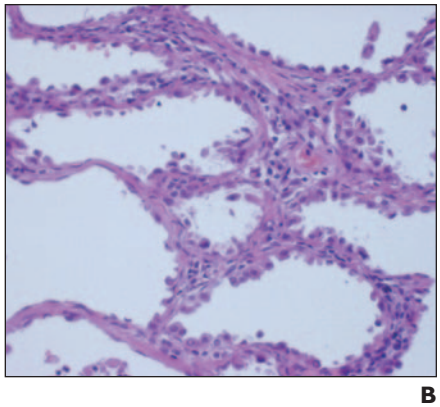

B

Fig. 2—66-year-old woman with atypical adenomatous hyperplasia.
A, Pure ground-glass opacification (diameter, 16 mm) in right upper lobe is seen on high-resolution CT image.
B, Histologically, atypical cuboidal pneumocytes extend along thickened alveolar septa.

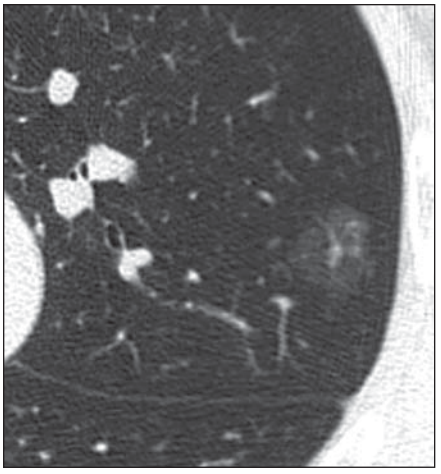

A

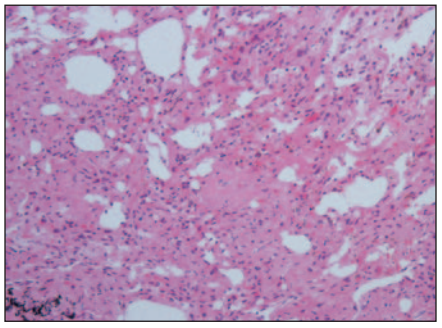

B

Fig. 3—74-year-old man with focal fibrosis.
A, High-resolution CT image shows pure ground-glass opacification (diameter, 17 mm) in left upper lobe preserving involved bronchiole and vascular structure.
B, Histologically, focal fibrosis with atelectasis and infiltration of inflammatory cells is present.

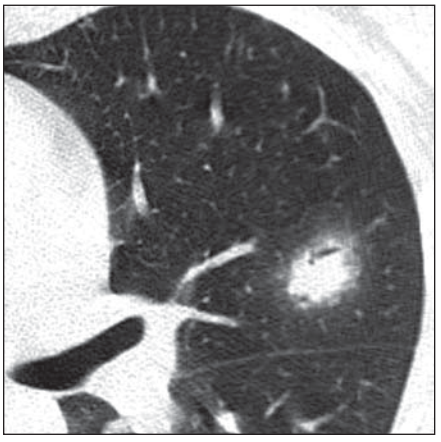

Fig. 4—28-year-old woman with invasive aspergillosis. Patient had leukemia and was treated with chemotherapy. High-resolution CT image shows nodule with air bronchogram and halo sign (diameter, 18 mm) in left upper lobe.

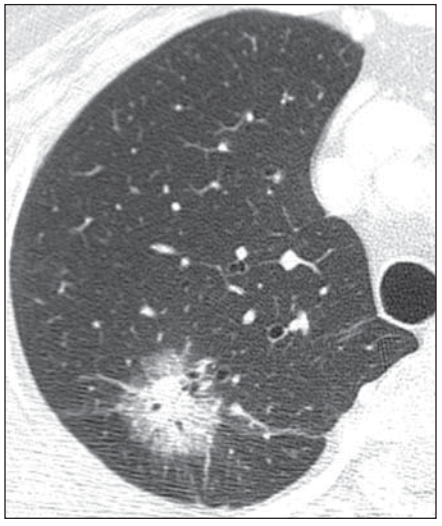

A

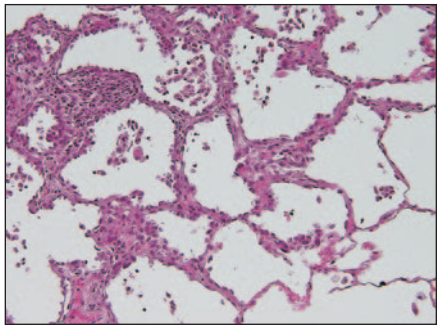

B

Fig. 5—63-year-old woman with minimally invasive adenocarcinoma.
A, High-resolution CT image shows nodule (diameter, 25 mm) with air bronchiologram in right upper lobe. Nodular margin is accompanied by zone of ground-glass attenuation (halo sign).
B, Pathologically, tumor cells extend widely along alveolar wall in outer zone of tumor.

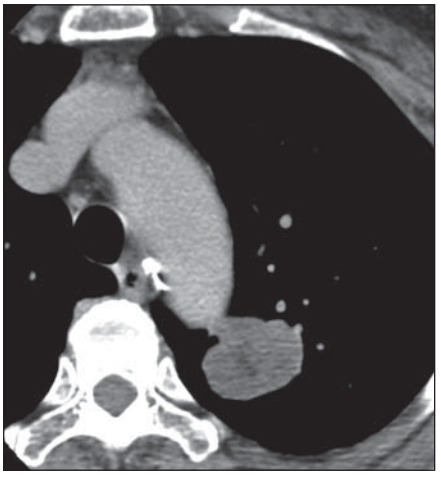

A

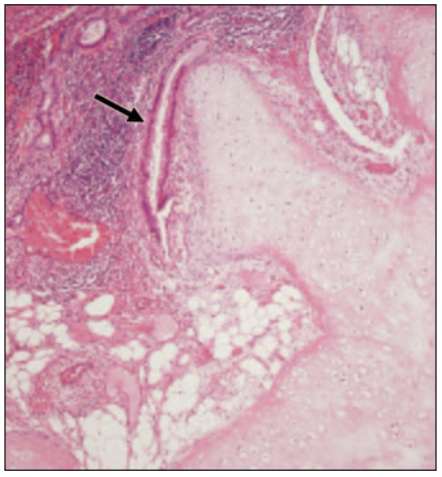

B

Fig. 6—65-year-old woman with hamartoma.
A, Contrast-enhanced target CT image at mediastinal window shows lobulated nodule (diameter, 28 mm) with low-attenuation component in left upper lobe. Low-attenuation area in nodule is not as low as that of fat, resembling primary lung cancer with degeneration and necrosis.
B, Histology shows nodule composed of cartilage, fat, and other mesenchymal structures. Arrow indicates slitlike cleft lined by ciliated epithelium.

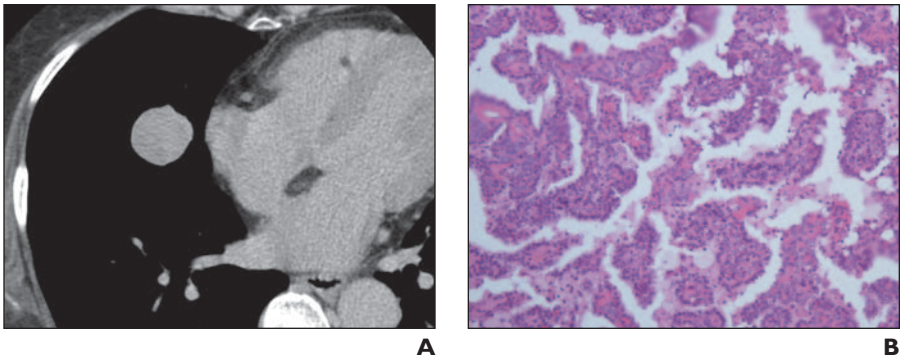

Fig. 7—72-year-old woman with pneumocytoma.
A, Contrast-enhanced target CT image at mediastinal window in equivalent phase shows homogeneously enhanced solid round nodule (diameter, 25 mm) in right middle lobe. Patient underwent surgery on suspicion of primary lung cancer.
B, Specimen shows cuboidal cells arranged in papillary or solid pattern. Nuclear atypia is not found. There are also sclerotic area and angiomatoid area in specimen (not shown). Diagnosis was ppneumocytoma.

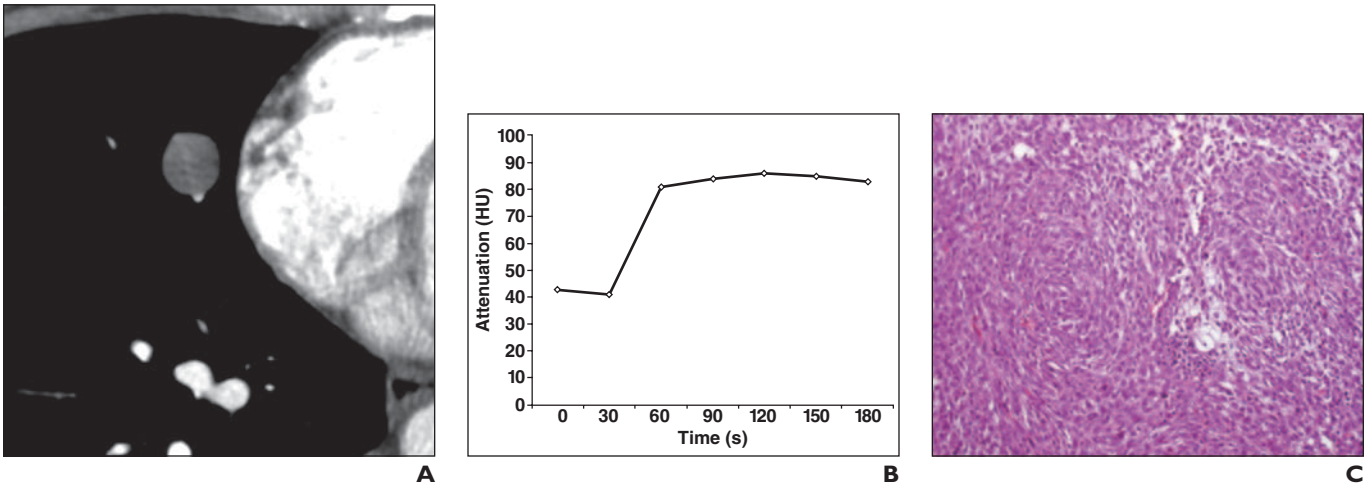

Fig. 8—42-year-old woman with asymptomatic inflammatory myofibroblastic tumor.
A, Contrast-enhanced CT image shows round nodule (diameter, 16 mm) in right middle lobe.
B, Graph of dynamic CT study shows early enhancement and maintains high attenuation until equivalent phase. Tumor shows intermediate signal intensity on T1-weighted image, high signal intensity on T2-weighted image, and is well enhanced on gadolinium-enhanced MRI (not shown). Maximum standardized uptake values in early and late phase ^{18}F-FDG PET study were 8.87 and 11.34, respectively (not shown). Surgery was performed on suspicion of malignancy.
C, Surgical specimen shows proliferation of spindle cells with marked inflammatory infiltrate and vascular proliferation with H and E stain. It was positive for vimentin, *CD68*, and anaplastic lymphoma kinase (not shown). Inflammatory myofibroblastic tumor was diagnosed.

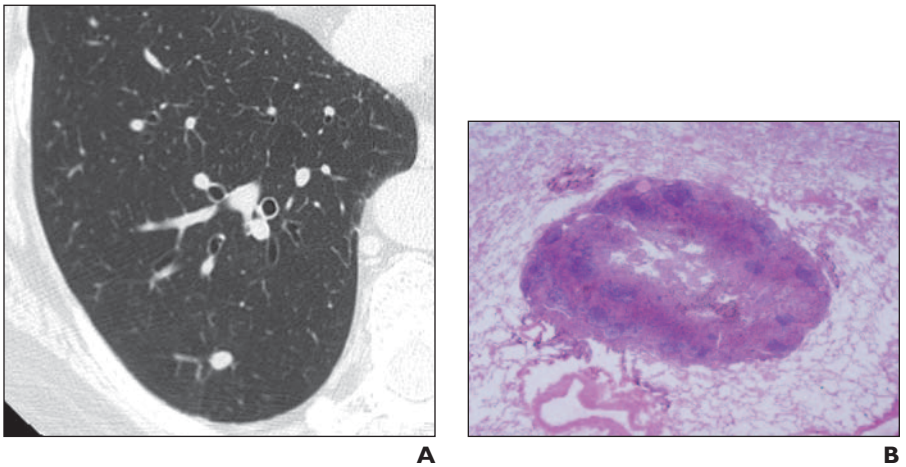

Fig. 9—69-year-old woman with intrapulmonary lymph node.
A, CT image shows well-demarcated oval nodule (diameter, 7 mm) in right lower lobe.
B, Specimen shows intrapulmonary lymph node with multiple lymphoid follicles.

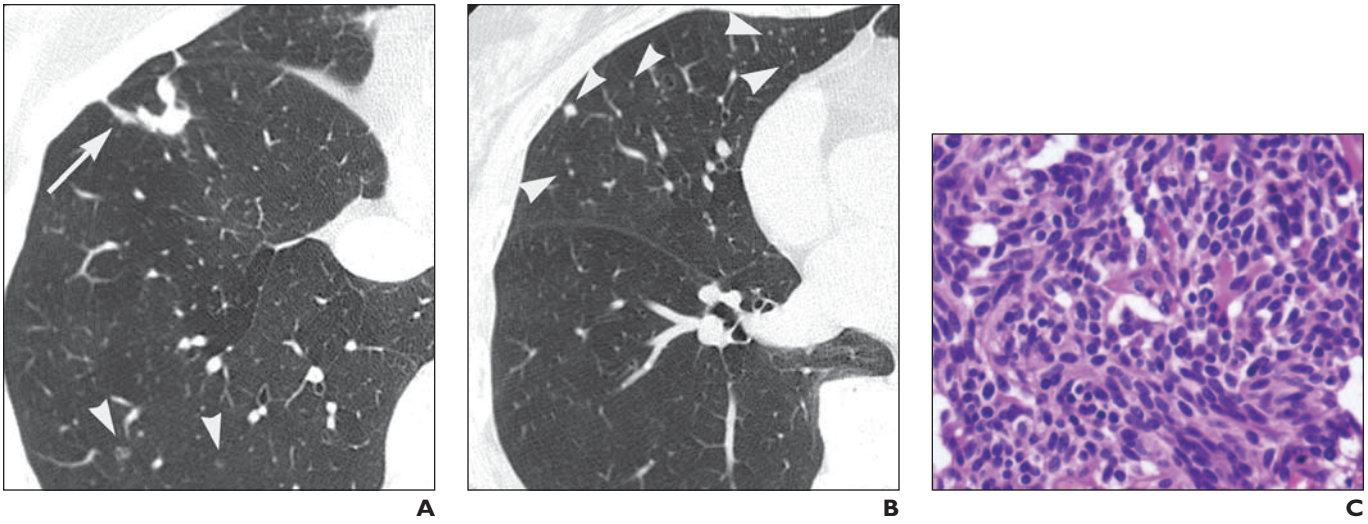

Fig. 10—61-year-old woman with pulmonary tumorlets.
A and **B,** Polygonal nodule (diameter, 20 mm) (*arrow*, **A**) in right lower lobe and multiple tiny nodules (diameter, 1–3 mm) (*arrowheads*, **A** and **B**) in right middle and lower lobe are shown on high-resolution CT images. Video-assisted thoracic surgery was performed for histologic examination.
C, Polygonal nodule revealed nontuberculous mycobacteriosis granuloma (not shown). Multiple tiny nodules were composed of polygonal or spindle cells with fibrous stroma. Tumor cells were positive for *CD56*, chromogranin, and epithelial membrane antigen (not shown). Granules of tumor cells were positive on Grimelius stain. Neuroendocrine granules were found on electron microscopy. Diagnosis was tumorlets associated with nontuberculous mycobacteriosis.

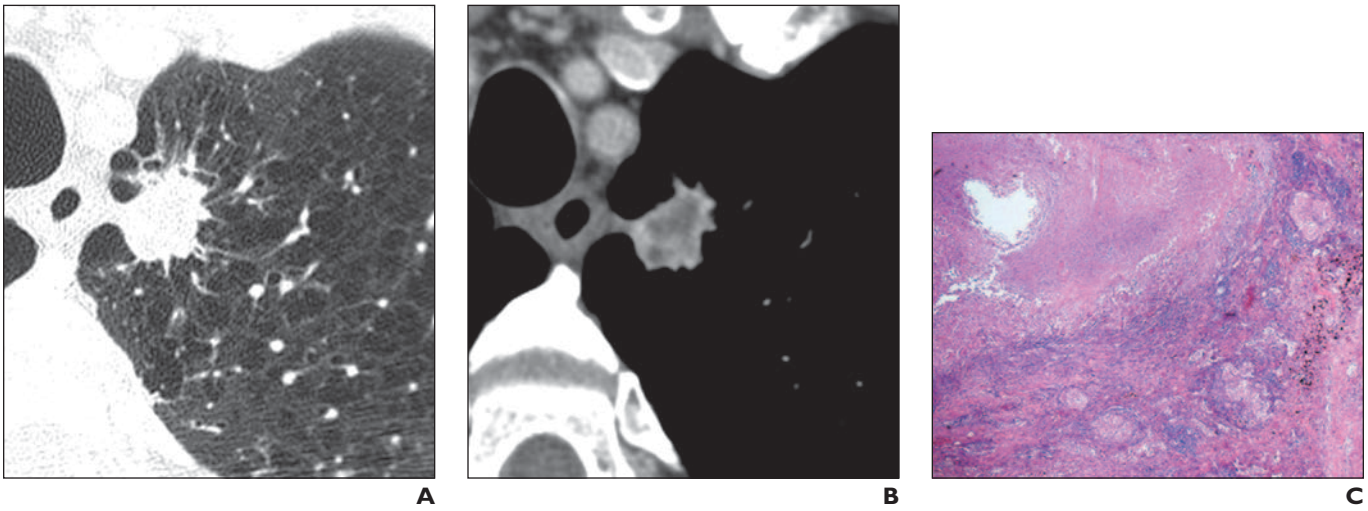

Fig. 11—73-year-old man with asymptomatic tuberculoma.
A, High-resolution CT image at pulmonary window shows nodule (diameter, 19 mm) in left upper lobe. Nodule has many fine spiculations mimicking primary lung cancer. Surrounding parenchyma is emphysematous.
B, Mediastinal window image shows heterogeneous low-attenuation area inside nodule in contrast with enhanced margin. Patient underwent video-assisted thoracoscopic surgery on suspicion of primary lung cancer.
C, Pathologic examination shows epithelioid granuloma with caseous necrosis. Diagnosis was tuberculoma.

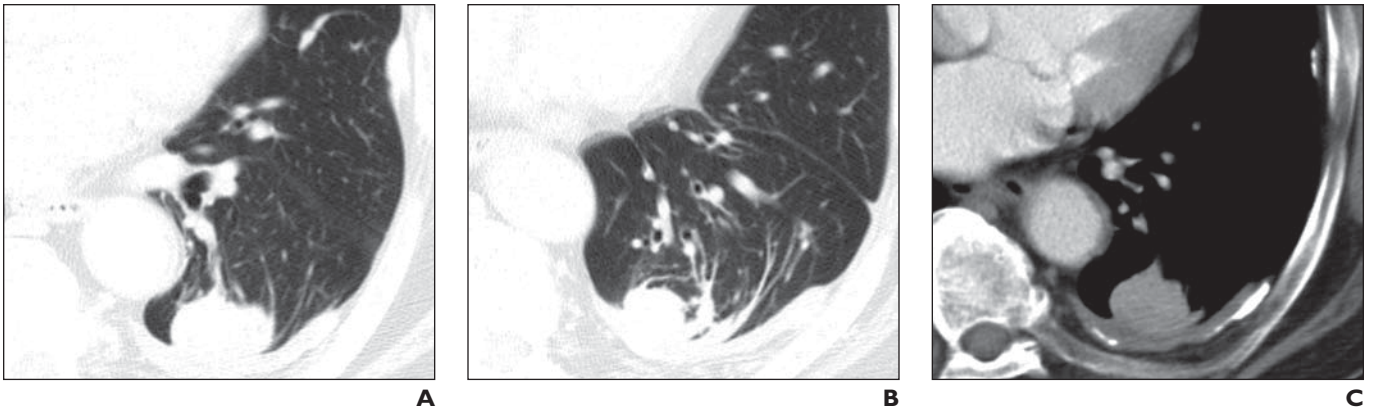

Fig. 12—74-year-old man with asymptomatic rounded atelectasis.
A, CT image shows pleural-based solid mass with spiculations (diameter, 31 mm) in left lower lobe mimicking lung cancer.
B, Contiguous image shows pulmonary vessels and bronchi curving into mass (comet-tail sign) that help to make correct diagnosis.
C, Contrast-enhanced CT image shows homogeneous enhancement. Mass widely contacts with thickened pleura with calcification. Rounded atelectasis was diagnosed.

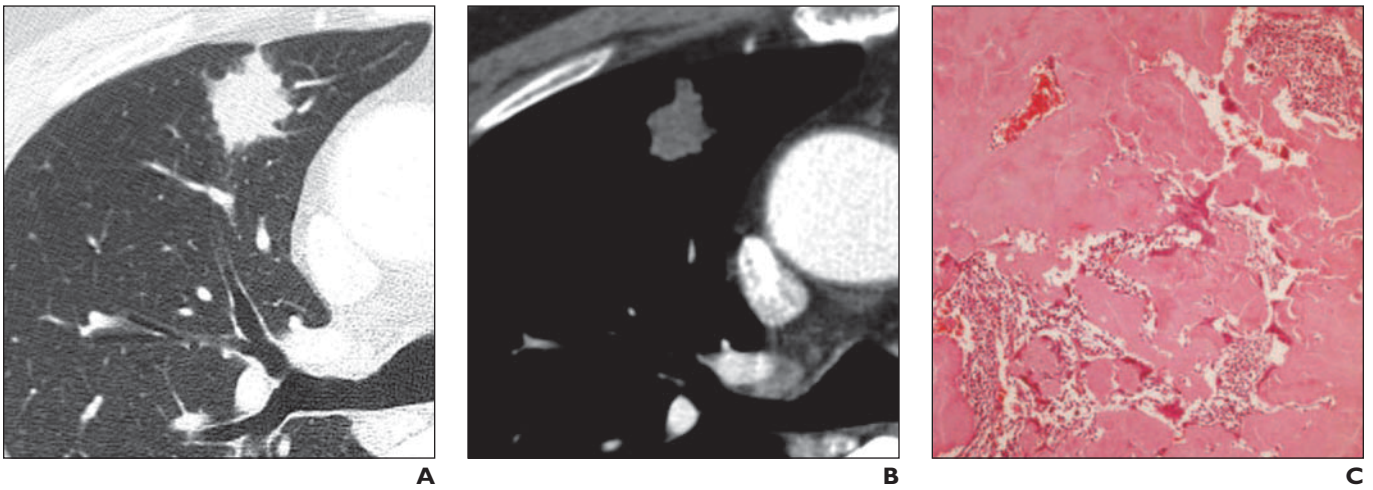

Fig. 13—69-year-old man with asymptomatic pulmonary amyloidosis.
A, Thin-section CT image at pulmonary window shows nodule with serrated margin (diameter, 23 mm) in right middle lobe mimicking primary lung cancer.
B, Nodule shows relatively poor enhancement on contrast-enhanced CT image.
C, Pathologic examination image shows that nodule comprised amorphous eosinophilic deposits.

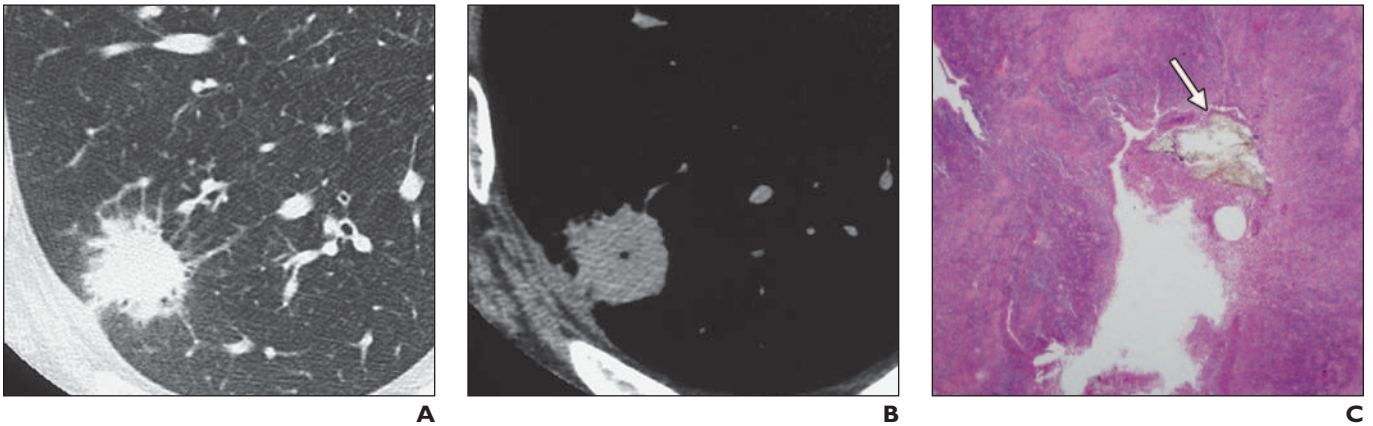

Fig. 14—60-year-old man with lung abscess due to aspiration of foreign body.
A, High-resolution CT image shows nodule (diameter, 28 mm) with fine spiculations and pleural indentation in periphery of right lower lobe.
B, Mediastinal window image shows small cavity in center of nodule.
C, Specimen image shows parenchymal defect surrounded by marked infiltration of chronic inflammatory cells. Arrow indicates alimentary fiber. Lung abscess due to foreign body aspiration was diagnosed.

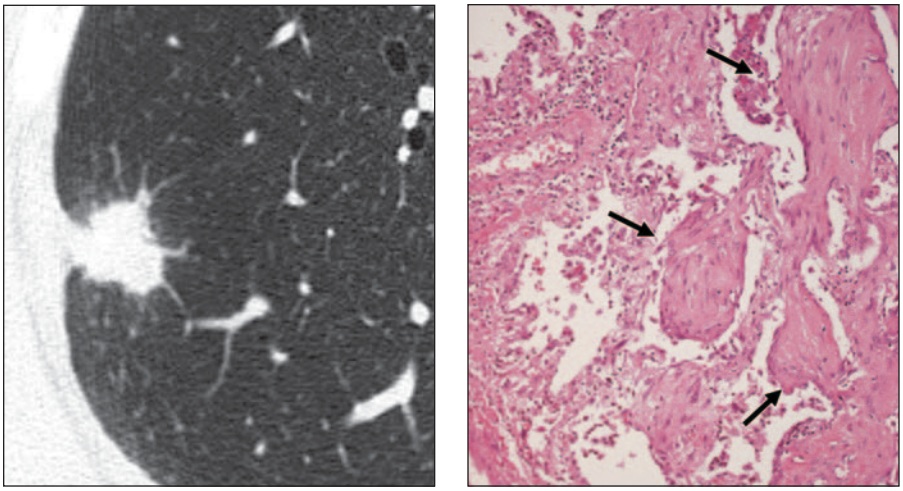

Fig. 15—60-year-old man with asymptomatic focal organizing pneumonia.
A, High-resolution CT image shows solid nodule (diameter, 25 mm) with serrated margin and rough spiculations in periphery of right lower lobe. Convergence of peripheral vessels and pleural indentation are also shown. He underwent video-assisted thoracoscopic surgery on suspicion of primary lung cancer.
B, Histology image reveals fibrotic foci with fibroblast proliferation, chronic inflammatory infiltrate, and dilated regenerative alveolar spaces containing fibrinous exudate admixed with inflammatory infiltrate (*arrows*). Focal organizing pneumonia was diagnosed.

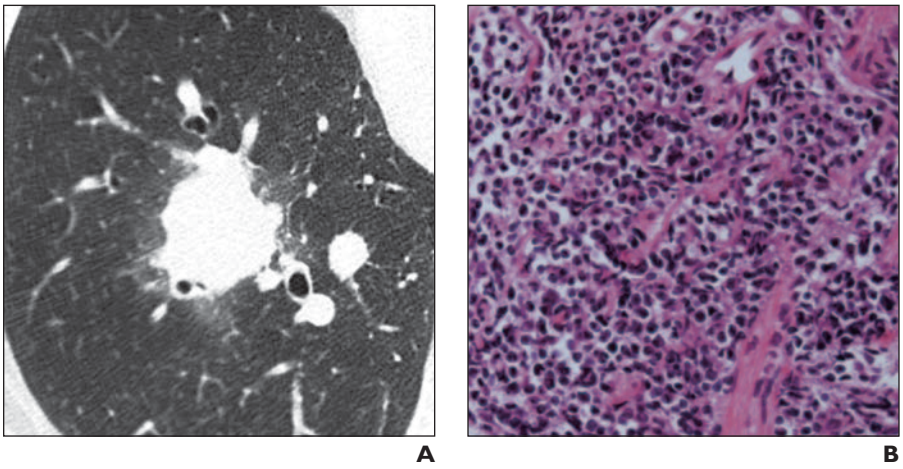

Fig. 16—73-year-old woman with secondary lymphoma who had been treated for non-Hodgkin follicular lymphoma.
A, CT image shows solid mass (diameter, 32 mm) with lobulated margin and ground-glass opacification component along bronchovascular bundle that resembles primary lung cancer.
B, Specimen image obtained by transbronchial lung biopsy shows marked infiltration of small cells with cellular atypia. Pulmonary involvement of lymphoma was diagnosed.